SCENARIOS FOR CIRCULAR GAMMA-GAMMA HIGGS FACTORIES

R. Aleksan, CEA Saclay, Paris, France; A. Apyan, Northwestern U., Evanston, USA;
Y. Papaphilippou, F. Zimmermann, CERN, Geneva, Switzerland

Abstract

The Higgs boson can be produced directly in gamma-gamma collisions generated by laser Compton back scattering off 80-90 GeV electron or positron beams. We discuss options for realizing a gamma-gamma Higgs factory using a high-energy circular e+e- collider, and/or its top-up injector ring, and compare the parameters and advantages of such a facility, including the expected performance, with those for a Higgs factory based on a recirculating linac, such as SAPPHiRE.

MOTIVATION

Even if no new unexpected finding is unveiled by the coming LHC Run 2, the evidence for non-baryonic dark matter, the cosmological baryon-antibaryon asymmetry and non-zero neutrino masses call for physics beyond the Standard Model. New particle accelerators are necessary to explore this physics. At present two design studies are underway for large accelerator complexes, i.e. the global Future Circular Collider (FCC) study [1] and the Chinese CepC/SppC [2]. In this paper we explore the possibility to realize a γγ collider Higgs factory based on the infrastructure of a future circular lepton collider, considering the example of the FCC-ee. A γγ Higgs factory can be realized by back-scattering two counter-propagating focused 80-90 GeV electron bunches off a laser pulse some ~1 mm before the e^-e^- collision point so that the backscattered γ's collide with a small spot size.

PRINCIPLE

In case the FCC-ee is used as the basis for such a γγ collider, the necessary electron bunches can be extracted from the two rings of the FCC-ee collider, one of which would need to have a magnet polarity opposite to the one required for its (e+) operation in the e+e^- collision mode. For the γγ option, we consider only e-beams since the luminosity will crucially depend on the rate at which the particle beams can be produced and accelerated. Generating a sufficient rate of positrons would be challenging. At a beam energy of 80-90 GeV about 4000 bunches per beam can be stored in the two collider rings, with a bunch intensity corresponding to ~100 MW of synchrotron radiation in total. After injection an initial synchrotron-radiation damping period of about 1000 turns (about two transverse amplitude damping times) is granted to establish the equilibrium emittances. Then one bunch per turn is extracted and collided in a dedicated bypass $\gamma\gamma$ interaction line with a bunch taken from the other beam; see Fig. 1.

Since the FCC-ee design features a single booster injector [3,4], which, in this application, would also need to switch polarity for injecting into one or the other ring, we can consider a cycle pattern, where one ring is half empty when the injection for the second ring takes place. The cycle is illustrated in Fig. 2, for a booster period of 1 s, and a booster-field ramp rate close to 500 G/s (corresponding to ~170 GeV/s, comparable to the SPS energy-ramp rate for the CNGS beam). For this cycle, the maximum total synchrotron radiation power in the two collider rings is only 3/4 of the amount one would expect when filling both rings completely.

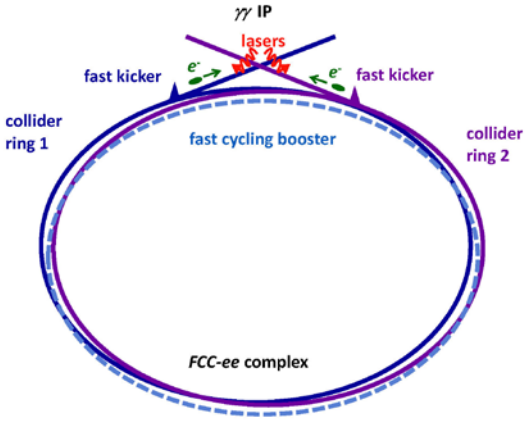

Figure 1: Schematic γγ collider based on filling the two FCC-ee collider rings with e^- bunches and extracting one bunch per beam and per turn into a dedicated γγ line.

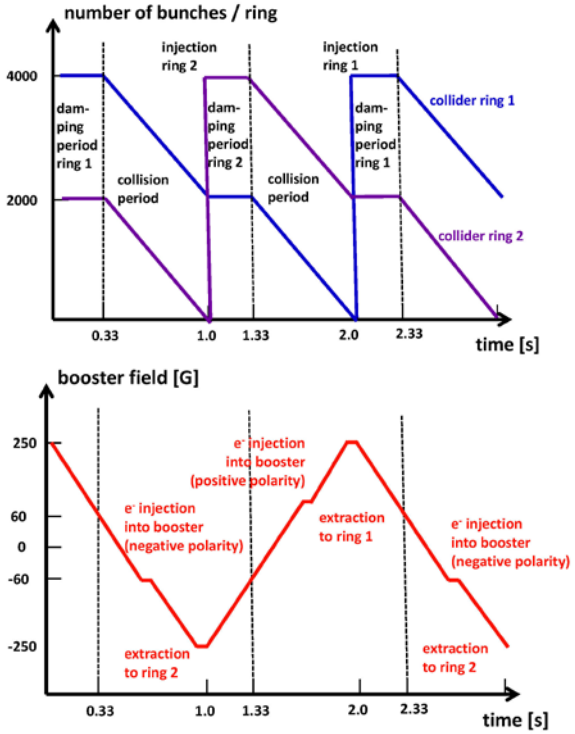

Figure 2: Cycle pattern for the two collider rings (top) and for the fast cycling booster (bottom). The injection energy is taken to be 20 GeV.

BEAM PARAMETERS AND POWER

The geometric e^-e^- luminosity is given by

$$L_{ee} = \frac{f_{rep} {N_b}^2}{4\pi\sqrt{\varepsilon_x \varepsilon_y \beta_x^* \beta_x^*}} F(\theta_c, \beta_y^*, \sigma_z, \sigma_x^*)$$

where $f_{\rm rep}$ denotes the average collision rate (2 kHz), N_b the bunch population, and F the geometric loss factor due to both crossing angle and hourglass effect. The $\gamma\gamma$ collisions are realized by Compton back-scattering at conversion points (CPs) located about 1 mm upstream of the interaction point [5]. We assume that the electron bunches are rotated by crab cavities. The electron beam crabbing is then inherited by the back-scattered photons. In this case the geometric luminosity loss is primarily due to the hourglass factor, given by [6]

$$F_{hg} = F(\theta_c = 0) = \sqrt{\frac{2}{\pi}}\, a\, e^{a^2} K_0(a^2) \text{ with } \equiv \frac{\beta_y^*}{\sqrt{2}\sigma_z}.$$

Figure 3 illustrates that σ_z should be smaller than $\sim 5\,\beta_y^*/\sqrt{2}$ (or $\sigma_z < 350\ \mu$m for $\beta_y^* \sim 100\ \mu$m) in order not to lose more than 40% in geometric luminosity.

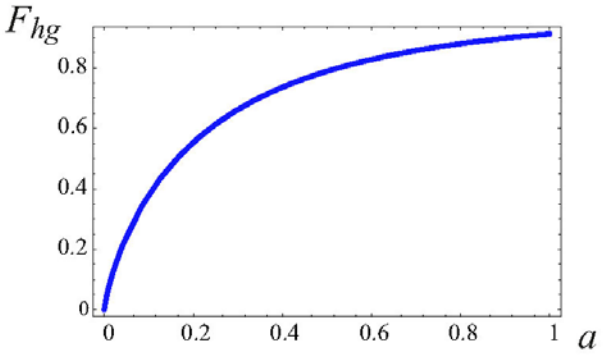

Figure 3: Hourglass reduction factor F_{hg} versus a.

In order to maximize the e^-e^- luminosity we now assume the same lowest-emittance optics as considered for operation at the top-quark energy (350 GeV c.m.) [7], and, therefore, scale the geometric emittances $\varepsilon_y, \varepsilon_x$ as the square of the energy, yielding 0.4 and 400 pm, respectively, at 80 GeV beam energy.

The rms energy spread is determined solely by the bending radius, $\rho \sim 10.6$ km [8], and the beam energy, $E \sim 85$ GeV (or $\gamma_{\rm rel} \sim 1.66\times10^5$) as [9] $\sigma_\delta = \gamma\sqrt{C_q/(\rho J_\epsilon)} \approx 0.07\%$ where $C_q = 3.84\times10^{-13}$ m denotes the quantum constant, and $J_\varepsilon = 2$ the longitudinal damping partition number. The rms bunch length follows as

$$\sigma_z = c\sqrt{\frac{m_e c C_q \alpha_c C \gamma^3}{2\pi J_\epsilon \rho e V_{rf} f_{rf}}}$$

where C signifies the circumference (taken to be 100 km) and α_c the momentum compaction factor, which has a value of 5.7×10^{-6} [10]. With an RF voltage to 12 GV, as for the FCC-ee t-tbar running) and assuming an RF frequency of 800 MHz we find $\sigma_z \approx 346$ μm, for which the hourglass loss factor $F_{hg} \sim 0.56$ may be just acceptable. The remaining luminosity loss could further be mitigated with a traveling focus scheme [11], e.g. by subjecting the electron bunches to a properly tuned rf quadrupole.

Considering a beam energy of 85 GeV, a bending radius of 10.6 km, a total SR power of 100 MW (sum of the two rings), and the cycle of Fig. 2, the maximum beam intensity per ring is 3×10^{14} electrons. Distributing this over 4000 bunches results in a bunch population of 7.7×10^{10}, and the equivalent geometric e^-e^- luminosity becomes 1.3×10^{34} cm^{-2}s^{-1} – without traveling focus. The average electron current required from the pre-injector complex is a moderate 50 μA.

Electric power is needed mainly for the RF system to compensate losses from synchrotron radiation and during acceleration. We can estimate these two contributions as follows. On average there are 3333 bunches in the two collider rings, each with 7.7×10^{10} electrons. Scaling from the FCC-ee design, the energy loss per turn is about 0.42 GeV Therefore the average synchrotron radiation power in the two collider rings amounts to 50 MW, with a peak of 93 MW (with the maximum number of 6000 bunches present). Accelerating 3×10^{14} electrons at 160 GeV/s requires an RF power close to 8 MW.

LASER PARAMETERS

The laser wavelength is chosen as 350 nm, since for an 80-90 GeV beam and near head-on laser-beam collisions this corresponds to a Compton x parameter close to 4.8, which is considered the optimum [5], since it results in the maximum energy of the back-scattered photons without yet allowing for pair production.

The average laser power required for FCC-ee is more relaxed than for SAPPHiRE [12,13]. It stays well within the parameter range targeted by ICAN [14-15] and in the reach of near-future technology [16].

SIMULATED $\gamma\gamma$ LUMINOSITY

Computer simulations with the code CAIN [17] have been performed tracking 75,000 and 400,000 (macro-) electrons per bunch, and considering an electron beam energy of 85 GeV, an rms electron bunch length of 0.35 mm, 100% laser polarization, as well as 80% electron-beam polarization. Figure 4 shows the simulated luminosity spectra for different values of the crossing angle between electron bunch and laser at the Compton conversion point. A crossing angle of 20 mrad does not lead to any noticeable luminosity degradation. Figure 5 presents spectra for different distances between the Compton conversion point and the $\gamma\gamma$ interaction point, indicating that a 1 mm distance is close to optimum.

Similar scans have determined the optimum Rayleigh length of the laser beam (z_R=0.3 mm, where the rms size of the laser beam at the CP equals $\sigma_{\gamma;x,y} \approx \sqrt{\lambda_\gamma z_R/(2\pi)}$), the optimum laser pulse length (0.15 mm rms), and the optimum laser flush again (5 J). The optimum parameters for the "FCC-γγ" are summarized in Table 1, which also compares with the corresponding values for SAPPHiRE.

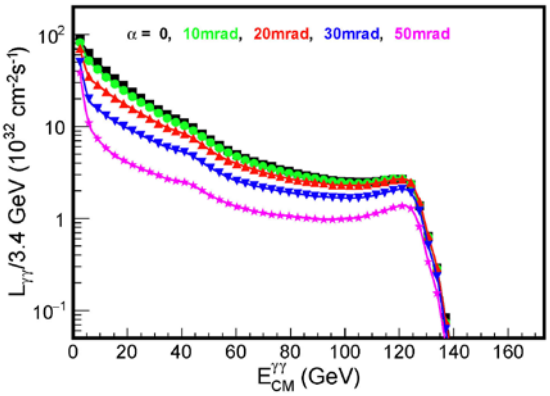

Figure 4: Simulated γγ luminosity per 3.4 GeV bin. The various curves refer to different e^-/laser crossing angles.

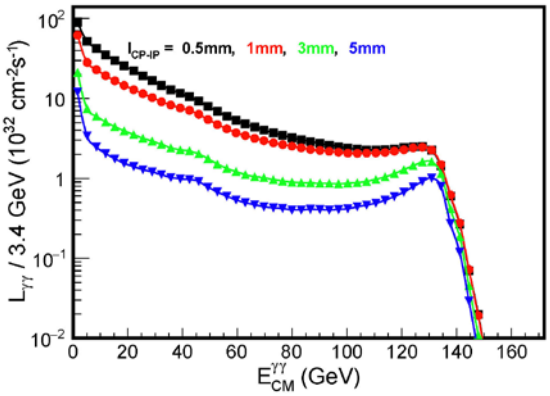

Figure 5: Simulated γγ luminosity per 3.4 GeV bin. The various curves correspond to different CP-IP distances.

The total FCC γγ luminosity is 3×10^{34} cm^{-2}s^{-1}. The differential luminosity (Figs. 4 and 5) assumes a local maximum close to the Higgs energy ($M_H c^2$≈125 GeV) of 2.5×10^{32} cm^{-2}s^{-1} (or 2-3× lower for unpolarised electrons).

The total number of Higgs bosons from the reaction $\gamma\gamma\rightarrow H$ can be estimated using the differential luminosity spectrum and a Breit-Wigner cross section

$$\sigma_{\gamma\gamma\rightarrow H} = 8\pi \frac{\Gamma(H\rightarrow\gamma\gamma)\Gamma_H}{\left(s_{\gamma\gamma} - {M_H}^2\right)^2 + {M_H}^2{\Gamma_H}^2}(1+\lambda_1\lambda_2)\,,$$

where $\Gamma(H\rightarrow\gamma\gamma)$ and Γ_H are the di-photon and total decay widths of the Higgs boson (about 8 keV and 4 MeV, respectively, in the Standard Model), and λ_1, λ_2 the initial photon helicities ($\lambda_1\lambda_2 = 1$). The cross section at the Higgs energy then has a peak value $\sigma_{\gamma\gamma\rightarrow H} \approx 2.5$ nbarn. Convoluted with the simulated wide luminosity spectrum, at FCC-γγ about 10000 Higgs bosons are produced in the $\gamma\gamma\rightarrow H$ process for a total effective integrated time of 10^7 s per year.

CONCLUSIONS

The FCC-ee complex can also be used as a γγ collider for direct Higgs production (Figs. 1 and 2). Preliminary parameters are shown in Table 1. With a wall-plug power comparable to the FCC-ee collider, and laser parameters similar to those foreseen by ICAN, up to 10,000 Higgs bosons could be produced per year.

This work was supported, in part, by the European Commission under the FP7 Capacities project EuCARD-2, grant agreement 312453.

Table 1: Tentative parameters for FCC-ee based γγ Higgs factory compared with those of SAPPHIRE.

	symbol	SAPPHIRE	FCC-ee
average el. power	P	100 MW	100 MW
beam energy	E	80 GeV	85 GeV
b. polarization	P_e	0.80	0.80
bunch popul.	N_b	10^{10}	7.7×10^{10}
laser rep rate	f_{rep}	200 kHz	3 kHz
av. collision rate	f_{coll}	200 kHz	2 kHz
laser pulse energy		5 J	5 J
laser power		1000 kW	15 kW
laser wave length	λ	350 nm	350 nm
Rayleigh length	z_R	0.3 mm	0.3 mm
rms laser spot CP	$\sigma_{\gamma;x,y}$	4 μm	4 μm
laser pulse length	σ_λ	0.25 mm	0.15 mm
# bunches / beam	n_b	-	4000
collider period		-	2 s
bunch length	σ_z	30 μm	350 μm
E damping time	τ_E	-	67 ms
energy spread	σ_δ	?	7×10^{-4}
RF frequency	f_{rf}	800 MHz	800 MHz
RF voltage	V_{rf}	2×10 GV	6 GV
γγ crossing angle	θ_c	≥20 mrad	≥20 mrad
nor.hor./vert. emit	$\gamma\varepsilon_{x,y}$	5, 0.5 μm	69, 0.06 μm
geom. h./v. emit.	$\varepsilon_{x,y}$	32, 3 pm	440, 0.4 pm
hor. IP beta funct.	β_x^*	5 mm	1 mm
vert. IP beta funct.	β_y^*	0.1 mm	0.1 mm
hor. rms spot size	σ_x^*	400 nm	700 nm
vert. rms spot size	σ_y^*	18 nm	6 nm
hor. rms CP spot	σ_x^{CP}	410 nm	1000 nm
vert. rms CP spot	σ_y^{CP}	180 nm	60 nm
distance IP – CP		~1 mm	1 mm
e^-e^- geometric luminosity	L_{ee}	2.2×10^{34} cm^{-2}s^{-1}	1.3×10^{34} cm^{-2}s^{-1}
$\gamma\gamma$ luminosity >125 GeV	$L_{\gamma\gamma}$	6×10^{32} cm^{-2}s^{-1}	8×10^{32} cm^{-2}s^{-1}

REFERENCES

[1] FCC web site http://cern.ch.fcc; also see M. Benedikt, F. Zimmermann, "The Future Circular Collider Study," CERN Courier 28 March 2014.

[2] CEPC web site http://cepc.ihep.ac.cn/ ; also see E. Gibney, "China Plans Super Collider," Nature 511, 394–395 (24 July 2014).

[3] Y. Papaphilippou, "FCC-ee Injector," ICFA HF2014 workshop Beijing (2014)

[4] Y. Papaphilippou et al, "Design guidelines for the injector complex of the FCC-ee," IPAC'15, these proceedings.

[5] V.I. Telnov, "Principles of Photon Colliders," Nucl.Instrum.Meth. A355 (1995) 3-18

[6] K. Hirata, PRL 74 (1995) 2228

[7] J. Wenninger et al., "Lepton Collider Parameters," CERN-ACC-SPC-0003, v1.0 (2014)

[8] B. Haerer, "Challenges and Status of the FCC-ee Lattice Design," ICFA HF2014 workshop Beijing (2014).

[9] M. Sands, "The Physics of Electron Storage Rings," SLAC-121 (1970).

[10] B. Haerer et al., "First Considerations on Beam Optics and Lattice Design for the Future Electron-Positron Collider FCC-ee," IPAC'15, these proceedings.

[11] V. Balakin, in SLAC-405 (1992).

[12] S.A. Bogacz, J. Ellis, L. Lusito, D. Schulte, T. Takahashi, M. Velasco, F. Zimmermann, "SAPPHiRE : a small γγ Higgs Factory," arXiv:1208.2827 (2012)

[13] F. Zimmermann, O. Bruning, M. Klein, "The LHeC as a Higgs Boson Factory," Proc. IPAC'13 Shanghai

[14] W.S. Brocklesby et al., "ICAN as a New Laser Paradigm for High Energy, High Average Power Femtosecond Pulses," The European Physical Journal Special Topics, Vol. 223, 6 (2014) 1189-1195

[15] G. Mourou, B. Brocklesby, T. Tajima, J. Limpert, Nat. Photon. 7, 258 (2013)

[16] Laura Corner, "Fibre Lasers for Gamma Colliders," Eur. Phys. J. Special Topics 223, 1207–1211 (2014)

[17] K. Yokoya et al., "CAIN: Conglomérat d'ABEL et d'interactions nonlinéaires," Nucl.Instrum.Meth. A355 (1995) 107-110